Spontaneous Intermembrane Transfer of Various Cholesterol-Derived Hydroperoxide Species: Kinetic Studies with Model Membranes and Cells†

Andrew Vila,‡ Witold Korytowski,‡,§ and Albert W. Girotti*,‡

Department of Biochemistry, Medical College of Wisconsin, Milwaukee, Wisconsin 53226, and Institute of Molecular Biology, Jagiellonian University, Krakow, Poland

Received July 6, 2001

ABSTRACT: Whereas spontaneous and protein-mediated transfer/exchange of cholesterol (Ch) between membranes has been widely studied, relatively little is known about the translocation of Ch oxidation products, particularly hydroperoxide species (ChOOHs), which can act as cytotoxic prooxidants. A major aim of the present study was to examine and compare the intermembrane transfer characteristics of several biologically relevant ChOOH isomers, including singlet oxygen-derived 5α-OOH, 6α-OOH, and 6β-OOH and free radical-derived 7α-OOH and 7β-OOH. These species were generated in [^{14}C]Ch-labeled donor membranes [erythrocyte ghosts or unilamellar DMPC/Ch (1.0:0.8 mol/mol) liposomes] by means of dye-sensitized photoperoxidation. Spontaneous transfer to nonoxidized acceptor membranes (DMPC liposomes or ghosts, respectively) at 37 °C was monitored by thin-layer chromatography with phosphorimaging radiodetection (HPTLC-PI) or liquid chromatography with mercury cathode electrochemical detection [HPLC-EC(Hg)]. The former allowed measurement of total (unresolved) ChOOH along with parent Ch, whereas the latter allowed measurement of individual ChOOHs. Ghost membranes in which ∼4% of the Ch had been peroxidized, giving mainly 5α-OOH, transferred total ChOOH and Ch to liposomes in apparent first-order fashion, the rate constant for ChOOH being ∼65 times greater. Like Ch desorption, ChOOH desorption from donor membranes was found to be rate limiting, and rate varied inversely with size when liposomal donors were used. For individual ChOOHs, rate constant magnitude (7α/7β-OOH > 5α-OOH > 6α-OOH > 6β-OOH) correlated inversely with reverse-phase HPLC retention time, suggesting that faster transfer reflects greater hydrophilicity. Liposome-borne ChOOHs exhibited the same order of toxicity toward COH-BR1 cells, which are deficient in ability to detoxify these peroxides. The prospect of disseminating oxidative cell injury via translocation of ChOOHs and other lipid hydroperoxides is readily apparent from these findings.

Phospholipids and unesterified cholesterol (Ch)[1] are known to move from one membrane compartment to another within cells in connection with membrane biogenesis and homeostasis (*1*−*4*). Numerous studies with membrane model systems have shown that phospholipids translocate extremely slowly on their own (i.e., without protein mediation), whereas Ch does so relatively rapidly (*1*, *2*). This might occur via random collisions of acceptor and donor membranes, although most of the experimental evidence to date favors a desorption/aqueous transit pool mechanism (*2*). Spontaneous transfer/exchange of Ch has been observed with acceptors such as unilamellar liposomes, red cell ghosts, lipoproteins, and mammalian cells (*2*, *3*). Transfer rate varies with factors such as relative polarity of the aqueous compartment and lipid packing density, degree of phospholipid unsaturation, and sphingomyelin level in the donor membrane (*2*). Altering the polarity of the sterol ring itself can also affect transfer efficiency. Thus, sitosterol (Ch with an ethyl group at the 24-position) translocates much more slowly than Ch (*5*), whereas oxidation products such as 7-ketocholesterol, 7α- or 7β-hydroxycholesterol, and 25-hydroxycholesterol all translocate more rapidly than Ch (*6*, *7*). The oxysterol behavior has been attributed more to weakened association with the membrane bilayer than to increased aqueous

† This work was supported by USPHS Grants CA72630 and TW001386 (to A.W.G.), KBN Grant 4P05A-068-16 (to W.K.), and NRSA Predoctoral Fellowship F31-CA85171 (to A.V.). This paper is based on research carried out by A.V. in partial fulfillment of the requirements for a Ph.D. degree in Biochemistry at the Medical College of Wisconsin.

* To whom correspondence should be addressed. Tel: 414-456-8432. Fax: 414-456-6510. E-mail: agirotti@mcw.edu.

‡ Medical College of Wisconsin.

§ Jagiellonian University.

[1] Abbreviations: $AlPcS_2$, aluminum phthalocyaninedisulfonate; BHT, butylated hydroxytoluene; BSA, bovine serum albumin; Ch, cholesterol; ChOOH(s), cholesterol hydroperoxide(s); DCP, dicetyl phosphate; DFO, desferrioxamine; DMPC, 1,2-dimyristoyl-*sn*-glycero-3-phosphocholine; GPX4, glutathione peroxidase isotype 4; HPLC-EC(Hg), high-performance liquid chromatography with mercury cathode electrochemical detection; HPTLC-PI, high-performance thin-layer chromatography with phosphorimaging detection; LOOH(s), lipid hydroperoxide(s); LUV(s), large unilamellar vesicle(s); PBS, Chelex-treated phosphate-buffered saline (125 mM NaCl, 25 mM sodium phosphate, pH 7.4); PBS/DFO, Chelex-treated PBS containing 0.1 mM DFO; POPC, 1-palmitoyl-2-oleoyl-*sn*-glycero-3-phosphocholine; SUV(s), small unilamellar vesicle(s); 5α-OOH, 3β-hydroxy-5α-cholest-6-ene 5-hydroperoxide; 6α-OOH, 3β-hydroxycholest-4-ene 6α-hydroperoxide; 6β-OOH, 3β-hydroxycholest-4-ene 6β-hydroperoxide; 7α-OOH, 3β-hydroxycholest-5-ene 7α-hydroperoxide; 7β-OOH, 3β-hydroxycholest-5-ene 7β-hydroperoxide; 7α/7β-OOH, undefined mixture of 7α-OOH and 7β-OOH.

10.1021/bi011408r CCC: $20.00
Published on Web 11/06/2001

solubility (*6*). Though little is known about the transfer properties of relatively stable oxysterols such as those mentioned, even less is know about cholesterol hydroperoxide (ChOOH) transfer. Like other lipid hydroperoxides (LOOHs) generated under oxidative stress conditions (*8*−*10*), ChOOHs can be deleterious to biomembrane structure/function on the basis of increased polarity alone (*8*, *9*). In addition (and possibly more importantly in some cases), ChOOHs can undergo iron-catalyzed one-electron reduction to free radical species which trigger damaging chain peroxidation reactions (*10*). Such reactions would radiate from the site of ChOOH origin on a given membrane. However, if peroxide movement to other membranes were possible, this could potentially expand the range of peroxidative damage, a prospect that has not been well appreciated up to now. In the case of ChOOHs, such translocation would be favored not only by greater polarity but also by a long lifetime compared with free radical precursors or products (*10*).

In an initial study testing the concept of LOOH delocalization (*11*), we showed that ChOOHs as a group move quite rapidly from one membrane to another and in so doing put the acceptor membrane at risk of free radical-mediated peroxidative injury. Using both model membranes and cells, we have now extended this work, comparing the transfer kinetics and cytotoxicity of several ChOOH isomers and testing the effects of variables such as ionic strength of the aqueous compartment and donor membrane size on transfer efficiency.

MATERIALS AND METHODS

Materials. Sigma Chemical Co. (St. Louis, MO) supplied the nonradioactive Ch, butylated hydroxytoluene (BHT), fatty acid-depleted bovine serum albumin (BSA), Chelex-100 (50−100 mesh), Dulbecco's modified Eagle's/Ham's nutrient F12 (DME/F12) medium, sterile trypsin−EDTA solution (10×), and trypan blue. 1,2-Dimyristoyl-*sn*-glycero-3-phosphocholine (DMPC) and 1-palmitoyl-2-oleoyl-*sn*-glycero-3-phosphocholine (POPC) were from Avanti Polar Lipids (Birmingham, AL). Hyclone Laboratories (Logan, UT) supplied the fetal calf serum, InvivoGen (San Diego, CA) the Plasmocin antibiotic, and Ciba-Geigy Corp. (Suffern, NY) the desferrioxamine (DFO). Aluminum phthalocyaninedisulfonate ($AlPcS_2$) was obtained from Dr. J. Van Lier (University of Sherbrooke) as a gift. $AlPcS_2$'s sulfonate groups are located on adjacent benzyl rings of the phthalocyanine macrocycle, making it an amphiphilic photosensitizer. ChOOH species, including 3β-hydroxy-5α-cholest-6-ene 5-hydroperoxide (5α-OOH), 3β-hydroxycholest-4-ene 6α-hydroperoxide (6α-OOH), 3β-hydroxycholest-4-ene 6β-hydroperoxide (6β-OOH), 3β-hydroxycholest-5-ene 7α-hydroperoxide (7α-OOH), and 3β-hydroxycholest-5-ene 7β-hydroperoxide (7β-OOH), were prepared by dye-sensitized photooxidation of Ch in pyridine solution or in liposomes (*12*−*14*). The different positional isomers were isolated by means of reverse- and normal-phase HPLC, and identities were confirmed by proton NMR, as described (*12*). Iodometrically determined ChOOHs (*14*) were stable for several months when stored in 2-propanol at −20 °C. [4-^{14}C]Ch (46 mCi/mmol in toluene) was obtained from Amersham Life Sciences, Inc. (Arlington Heights, IL). Before incorporation into SUVs or ghost membranes (see below), the [^{14}C]Ch was separated from any preexisting oxidation products by means of normal-phase HPLC (*11*); the Ch fraction was dried under argon at room temperature and used immediately. [*oleoyl*-1-^{14}C]POPC [58 mCi/mmol in toluene/ethanol (1:1 v/v)] was obtained from NEN Life Sciences, Inc. (Boston, MA) and used without further purification.

Liposome Preparation. Small unilamellar vesicles (50 nm SUVs) and large unilamellar vesicles (100 and 200 nm LUVs) were fabricated using an extrusion device (Lipex Biomembranes, Vancouver, BC) with polycarbonate filters of appropriate pore size (Nucleopore Corp., Pleasanton, CA). Details of the lipid preparation and extrusion process are described elsewhere (*12*). Most transfer experiments were carried out using 50 nm SUVs (with the highest surface/volume ratio) as acceptors or donors; the LUVs were used when effects of donor size on transfer rate were examined. Typical lipid compositions and bulk phase concentrations were as follows: (i) 10 mM DMPC/0.1 mM DCP (for measuring sterol transfer from ghost membrane donors); (ii) 2.0 mM DMPC/1.6 mM (1.0 μCi/mL) [^{14}C]Ch/0.04 mM DCP (for measuring sterol transfer from liposomal donors); (iii) 1.0 mM POPC/0.7 mM Ch/0.1 mM ChOOH/0.02 mM DCP (for comparing cytotoxic effects of different ChOOH isomers). The Ch content relative to phospholipid for SUV and LUV donors (~45 mol % Ch) approximates that of most natural plasma membranes (*15*). DCP (1 mol %) was included so as to impose a net negative charge on the liposome surface, thereby diminishing the possiblity of membrane contact/fusion during transfer experiments. A trace of [^{14}C]POPC (0.25 μM; ~15 nCi/mL) was typically included in SUV acceptor preparations, serving as an internal standard to correct for any sampling or extraction discrepancies. There was no significant translocation of this marker over the course of a typical transfer experiment. The aqueous phase for all liposome preparations was PBS that had been Chelex-treated (*16*) in order to deplete metal ions that might catalyze ChOOH decomposition and/or adventitious generation of peroxides (*17*). Liposomes were stored under argon at 4 °C and used within a 3-day period.

Erythrocyte Ghost Preparation and [^{14}C]Ch Labeling. Erythrocyte plasma membranes (unsealed ghosts) were prepared from human blood freshly drawn in the presence of 2 mM EDTA. Erythrocytes were pelleted, washed 3−4 times with PBS, and then lysed, using at least 60 volumes of ice-cold 5 mM phosphate, pH 8.0 (*18*). After centrifugation at 4 °C, the recovered membrane fraction was washed extensively with lysing buffer to remove hemoglobin and then with PBS/0.1 mM DFO/0.1 mM EDTA to deplete nonheme iron and other metal ions that might catalyze peroxide formation/turnover (*17*). Ghost preparations in PBS/0.1 mM DFO (PBS/DFO) were stored under argon at 4 °C and used for transfer experiments within 10−14 days. Total membrane protein was determined according to Lowry et al. (*19*), using 0.2% (w/v) sodium dodecyl sulfate for solubilization. Molar concentration of total lipid was based on published values of overall lipid composition and lipid/protein mass ratio (*20*). Immediately before being used as sterol donors in transfer experiments assessed by HPTLC-PI, ghost membranes were labeled with [^{14}C]Ch, using defatted BSA as an aqueous vehicle (*21*). The labeling procedure has been modified so as to require less than 1 h, thus resulting in relatively little autoxidation of the prepurified Ch; details are described elsewhere (*11*).

Cell Culture. COH-BR1 cells, an epithelial line derived from pleural effusion of a patient diagnosed with breast cancer (*22*), were obtained as a gift from Dr. James Doroshow, City of Hope Cancer Center. These cells were well suited for assessing cytotoxicity in relation to rate of 5α-OOH, 6-OOH, and 7-OOH transfer acquisition because they express little, if any, glutathione peroxidase isotype 4 (GPX4) (*22*, *23*), a selenoperoxidase which detoxifies these ChOOHs at different rates (*13*). Cells were grown in 75 cm^2 flasks under standard culture conditions (*22*), using DME/F12 supplemented with 10% fetal calf serum and 5 μg/mL Plasmocin as the growth medium. (Plasmocin protected against a broad-range of bacterial infections, including *Mycoplasma* infection.) The cells were given fresh medium in 2 day intervals and subcultured after reaching ~90% confluency, using 0.5% (w/v) trypsin/5 mM EDTA in PBS for detachment and diluting 6-fold with fresh medium prior to replating. Protein content of near-confluent cells, as determined by Bradford assay (*24*), was found to be 15.2 ± 1.2 mg/10^8 cells (mean ± SE, $n = 10$). Total lipid content was estimated to be 4.7 mg (6.3 μmol)/10^8 cells, based on protein content in relation to protein and lipid contents and compositions of other cell lines (*25*, *26*).

Photogeneration of ChOOHs in Donor Membranes. [^{14}C]-Ch-labeled ghost or SUV membranes were charged with ChOOHs via singlet oxygen-mediated photodynamic action, using $AlPcS_2$ as a sensitizing agent (*27*). A typical procedure for ghosts was as follows. The membranes (1.3 mg of protein/mL; 1.1 mg of lipid/mL or ~0.74 mM Ch) in PBS/DFO were sensitized with 20 μM $AlPcS_2$, placed in a 25 °C thermostated beaker, and then irradiated from above, using a quartz−halogen source; fluence rate measured at the reaction mixture surface was ~150 mW/cm^2. Other details were as described elsewhere (*14*, *17*). Liposome suspensions (e.g., SUVs at a concentration of 1.0 mM DMPC/0.8 mM Ch/0.02 mM DCP) were photooxidized similarly, but at 4 °C instead of 25 °C. The temperature-dependent isomerization of 5α-OOH to 7α-OOH (*28*) was more pronounced in liposomes than ghosts (*29*), and the lower temperature slowed this significantly so that the starting level of 5α-OOH was adequate for transfer measurements. ChOOH yields were determined by HPLC-EC(Hg) analysis (*14*, *30*). Ghost membranes and liposomes both exhibited a linear accumulation of ChOOHs out to at least 1 h of photooxidation, the rates being ~2 μM/min and ~0.67 μM/min, respectively. Photoperoxidized ghost preparations were washed twice with PBS/DFO to remove any membrane fragments and then used immediately for transfer measurements.

Sterol Transfer Conditions. When ChOOHs were generated by photooxidation of donor membranes, it was necessary to carry out transfer reactions in the dark in order to avoid further photoactivation of membrane-associated $AlPcS_2$. A typical reaction mixture for assessing sterol (ChOOH and Ch) transfer from ghosts to liposomes consisted of 0.4 mM total ghost lipid (5−10 μM as ChOOH), 2.7 mM total liposomal lipid, 10 μM BHT, and 0.5% ethanol (the BHT vehicle) in PBS/DFO; the final volume was 2.0 mL. (Concentrations in bulk suspension are indicated.) As a chain-breaking antioxidant, BHT was included to further reduce the possibility of new peroxide formation during transfer incubation. At the indicated concentrations, neither BHT nor ethanol had any significant effect on the ChOOH or Ch transfer kinetics (data not shown). The membrane mixtures in 13 × 100 mm Pyrex test tubes capped with glass marbles were incubated at 37 °C in a Pierce Reacti-Therm block. Periodically during incubation, the tubes were gently vortexed for 1−2 s. At various time points over a 90 min period (ChOOH transfer) or 24 h period (Ch transfer), a 175 μL sample was removed from each tube and diluted with an equal volume of ice-cold PBS to quench the reaction (*11*). After centrifugation at 4 °C (16000*g*, 10 min), a 175 μL aliquot from each supernatant (liposome-containing) fraction was mixed with 75 μL of PBS/1 mM EDTA and extracted with 0.4 mL of chloroform/methanol (2:1 v/v), as described (*14*, *31*). For determining total ChOOH or Ch, matching samples were quenched and extracted directly, i.e., without separaton of donor and acceptor membranes. Since changes in total sterol content were typcially very small, it was usually sufficient to take these samples at the beginning, middle, and end of a transfer incubation. A 0.2 mL aliquot from each organic phase was evaporated under a stream of N_2, and recovered lipid material was stored at −20 °C for subsequent HPTLC-PI or HPLC-EC(Hg) analysis, which was typically completed within 48 h. Data reflecting transfer acquisition of ChOOHs or Ch by liposomes were plotted according to the relationship:

$$\ln[(S_\infty - S_t)/(S_\infty - S_0)] = -k_a t \quad (1)$$

where S_0, S_t, and S_∞ represent acquired sterol at times zero, t, and infinity, respectively; and k_a is the first-order rate constant for acquisition. Sterol departure from ghosts under the conditions described was also monitored. In this case, the sample volume was reduced to 100 μL, and 250 μL of ice-cold PBS was used for quenching. After centrifugation, the ghosts were recovered, washed twice via resuspension in cold PBS with centrifugation, and finally resuspended in 250 μL of PBS/1 mM EDTA. Lipids were then extracted for HPTLC-PI or HPLC-EC(Hg) analysis. Data reflecting ChOOH or Ch departure from ghosts were plotted according to the relationship:

$$\ln(S_t/S_0) = -k_d t \quad (2)$$

where S_0 and S_t represent remaining sterol at times 0 and t, respectively; and k_d is the first-order rate constant for departure.

The above transfer arrangement was reversed in some experiments; i.e., photoperoxidized liposomes were used as donors and ghosts as acceptors. A typical reaction mixture in this case consisted of 60 μM total liposomal lipid (1−2 μM as ChOOH), 0.6 mM total ghost lipid, 10 μM BHT, and 0.5% ethanol in PBS/DFO. At various time points during transfer at 37 °C, a 200 μL sample was removed, quenched with an equal volume of cold PBS, and centrifuged. A 200 μL aliquot was drawn from the supernatant fraction, mixed with 50 μL of PBS/1 mM EDTA, and extracted (see above), the recovered ChOOHs being analyzed by HPLC-EC(Hg).

A typical procedure for examining cytotoxic ChOOH transfer from SUVs to COH-BR1 cells was as follows, sterile working conditions being maintained throughout. Cells were seeded into six-well culture plates at a titer estimated to give 80−90% confluency after approximately 2 days. The cells

were then washed free of growth medium and exposed to ChOOH-bearing SUVs in PBS containing 10 mM D-glucose, 0.9 mM $CaCl_2$, and 0.4 mM $MgCl_2$ (1.0 mL per well). Stock SUV preparations in this case were fabricated with individual ChOOHs and consisted of POPC, Ch, and 5α-OOH, 6β-OOH, or 7α-OOH (10:7:1 by mol; 1.8 mM total lipid in PBS). Before being added to cells, the SUV suspensions were sterilized, using 0.22 μm pore filters. In a typical experiment, each well (~1.3×10^6 cells) contained ~80 μM total cell lipid, 100 μM SUV lipid, and 5.5 μM ChOOH. Liposomes lacking ChOOH, i.e., POPC/Ch (10:8 mol/mol) SUVs, were used as controls to correct for any background cytotoxicity. At zero time and various other time points during incubation at 37 °C, an aliquot of SUV-containing medium was centrifuged to remove any detached cells (counted as nonviable; see below) and then extracted; recovered ChOOHs were determined by HPLC-EC(Hg). Concurrently, the cells remaining in each well were detached by brief exposure to 10-fold diluted trypsin−EDTA and then suspended in 1.0 mL of serum-containing medium. Immediately thereafter, the viable cell count was determined by trypan blue exclusion assay (*32*).

HPTLC-PI Analysis. Intermembrane transfer of [^{14}C]Ch and [^{14}C]ChOOH could be monitored simultaneously by means of normal-phase HPTLC with phosphorimaging (PI) detection. This approach afforded excellent separation of parent Ch from ChOOH species but relatively poor separation of the latter from one another (*11*, *33*). Consequently, the latter were examined collectively when this approach was used. High-performance silica gel 60 plates (10 × 20 cm; 0.2 mm layer thickness) were obtained from EM Science (Gibbstown, NY). Typical amounts of total lipid used for analysis were as follows: 110−120 nmol (when measuring sterol uptake by liposomes), 40−42 nmol (when measuring sterol departure from ghosts), and 6−7 nmol (when measuring sterol departure from liposomes). Each lipid extract was solubilized in 20 μL of hexane/2-propanol (97:3 v/v) and applied to the TLC plate in a hairline N_2 stream, using a Linomat IV programmable applicator from Camag Scientific, Inc. (Wilmington, NC). Chromatography was carried out in a 9 × 20 × 24 cm glass chamber, using benzene/ethyl acetate (1:1 v/v) as the mobile phase. The chamber was shielded from room light and any abrupt changes in ambient temperature. Average running time at 25 °C was ~15 min. After air-drying, the plate was analyzed for radioactive Ch and ChOOH (detection limit ~5 pmol), using a Storm 860 storage phosphor system (*34*) with ImageQuant 4.2 software (Molecular Dynamics, Sunnyvale, CA). Plates were developed at room temperature over a 36−48 h period. Ghost-to-SUV transfer rates, measured as percent sterol taken up by SUVs, were detrmined from the image intensity at each time point relative to that for whole samples (SUVs plus ghosts), correcting for any zero time signals due to ghost contamination. When included as a loading standard in SUV acceptors, [^{14}C]POPC remained near the origin, thereby not interfering with [^{14}C]Ch and [^{14}C]ChOOH signals.

HPLC-EC(Hg) Analysis. Reverse-phase HPLC with reductive mode electrochemical (EC) detection on a mercury drop was used to detect individual ChOOH species in ghost membranes and liposomes during transfer incubation. Chromatography was carried out using an Ultrasphere XL-ODS column (4.6 × 70 mm; 3 μm particles) from Beckman Instruments (San Ramon, CA), a Model 2350 HPLC pump with injection valve from Isco (Lincoln, NE), and a Model 420 electrochemical detector from EG&G Instruments, Inc. (Oak Ridge, TN). The detector is equipped with a renewable mercury drop electrode, which was set to operate at −150 mV vs a Ag/AgCl reference. Separations were carried out at room temperature, using a deoxygenated mobile phase composed of (by volume) 72% methanol, 11% acetonitrile, 8% 2-propanol, and 9% 1 mM sodium perchlorate in water. The mobile phase was purged of oxygen by bubbling with He (30 min), followed by Ar (1 h before and then throughout a chromatographic run). Dried lipid extracts from liposomes and ghost membranes were dissolved in 50 μL of 2-propanol, 10 μL of which was injected into the HPLC system. The elution flow rate was typically 1.0 mL/min. Other details were as described (*14*, *30*). Assignment and quantitation of EC peaks was based on the retention times and amperometric responses of ChOOH standards. The responsiveness of 5α-OOH was ~90% that of 7α/7β-OOH (unresolved 7α- and 7β-OOH) and ~25% greater than that of 6α- or 6β-OOH. Detection limits for these peroxides were in the 0.1−0.2 pmol range (*30*).

RESULTS

Comparison of ChOOH and Ch Transfer Kinetics. Initial experiments were carried out using photoperoxidized [^{14}C]-Ch-labeled erythrocyte ghosts as ChOOH donors and 50 nm DMPC/DCP (100:1 mol/mol) SUVs as acceptors. Lipid extracts of the SUV compartment during transfer incubation were analyzed by HPTLC with phosphorimaging detection, which afforded an excellent separation of parent Ch from the more polar ChOOH derivatives and any other oxidized forms that may have been present initially or generated during incubation (*11*, *33*). On the other hand, HPTLC permitted only a partial separation of individual ChOOH isomers. Consequently, the transfer behavior of the entire ChOOH population relative to Ch was examined in this phase of the work. Figure 1 shows an HPTLC-PI chromatogram depicting the progressive transfer at 37 °C of radiolabeled Ch and ChOOH from ghost donors to SUV acceptors, the latter existing in ~6.5-fold lipid molar excess over the former. The SUVs contained a trace of radiolabeled POPC (band near origin in Figure 1), which served as an internal standard to correct for any sample load inconsistencies. POPC itself translocated at a negligible rate (*2*) compared with ChOOH and Ch. For the Figure 1 experiment, which is representative of at least six other experiments involving HPTLC-PI analysis, variability in sample loading was <10%. Donor ChOOH at the outset of this particular experiment consisted mainly of 5α-OOH (~70%), with progressively smaller amounts of 6β-OOH, 7α/7β-OOH, and 6α-OOH, as determined by HPLC-EC(Hg) (see below). The Ch and ChOOH band signals at zero time are ascribed to a small amount of nonpelletable ghost material in the SUV fraction. When peroxidized ghosts were incubated for at least 4 h in the absence of SUVs, neither of these signals increased to any significant extent (results not shown), ruling out any time-dependent ghost fragmentation and contamination of the SUV fraction as a possible complication. Analysis of lipid extracts from the entire reaction system (SUVs, ghosts, and aqueous compartment) also revealed little, if any, change in either the ChOOH or Ch signal over at least a 4 h span

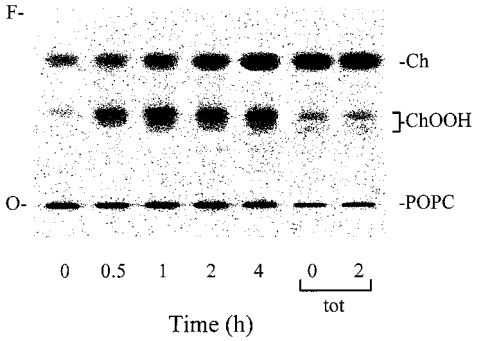

FIGURE 1: HPTLC-PI profile depicting progressive transfer of [^{14}C]-ChOOH and [^{14}C]Ch from ghost membranes to liposomal membranes. [^{14}C]Ch-labeled ghosts were photoperoxidized to a level of 28.6 μM total ChOOH in bulk suspension (~3.9% of the starting Ch concentration). The transfer incubation mixture consisted of photoperoxidized ghosts (178 μM [^{14}C]Ch, 7.2 μM [^{14}C]ChOOH; total radioactivity ~50 nCi/mL) and DMPC/DCP (100:1 mol/mol) SUV acceptors in PBS/DFO/10 μM BHT at 37 °C. [The SUVs contained a trace of [^{14}C]POPC (~0.8 nCi/mL), which served as a loading standard; POPC signal intensity averaged ~30-fold greater than background.] Total SUV lipid and ghost lipid concentrations were 2.70 and 0.41 mM, respectively (mol ratio ~6.5:1). At the indicated time points, samples were quenched with equal volumes of cold PBS and centrifuged. Aliquots from supernatant (SUV) fractions were extracted and recovered lipids subjected to HPTLC-PI analysis. Aliquots from noncentrifuged samples representing the entire reaction system (total) were examined alongside. Lipid analyzed: 174 nmol per lane (SUV fractions, 0−2 h); 58 nmol per lane (total, 0 and 4 h). The latter samples were scaled down for more accurate measuement of the relatively high radioactivity in the Ch band. The upper band in the ChOOH zone represents mainly 5α-OOH with a trace of unresolved 7β-OOH, whereas the lower band represents 7α-OOH and 6α/6β-OOH. O = origin; F = solvent front.

[Figure 1, total (*11*)]. This indicates that further peroxidation of Ch during transfer incubation and/or turnover of ChOOHs with formation of other oxidation products (*33*) was negligible under the conditions used. [For individual ChOOH species, this was confirmed by HPLC-EC(Hg) analysis; see below.] On the other hand, if lysing volumes for preparing ghost membranes were not large enough (see Materials and Methods), significant ChOOH losses would accrue during transfer (not shown), presumably because of greater hemin/methemoglobin retention (*18*). ChOOHs also degraded more rapidly if reactions were carried out in non-Chelexed PBS and chelators (DFO, EDTA) were omitted. It is apparent from Figure 1 that not only did Ch and ChOOHs translocate from ghosts to SUVs but the latter did so far more rapidly (note the faster increase in ChOOH signal intensity over the first 2 h). This was confirmed by quantitating the changes in HPTLC-PI band intensities for ChOOH and Ch over time (Figure 2). The plots in Figure 2A represent sterol fraction remaining in ghost membranes; those in Figure 2B represent sterol fraction acquired by SUVs in the same transfer system. These data clearly indicate that, on a fractional basis, departure from ghosts and uptake by SUVs occurred much more rapidly for the ChOOH population than for parent Ch. Reducing the reaction temperature from 37 to 4 °C slowed all transfer by >95% (results not shown). The greater hydrophilicity of ChOOH would have made desorption from the donor surface more favorable. Approximately 90% of the ChOOH appeared in the acceptor compartment at ~3 h, with little change thereafter, suggesting that an equilibrium state had been reached. This would have greatly favored the

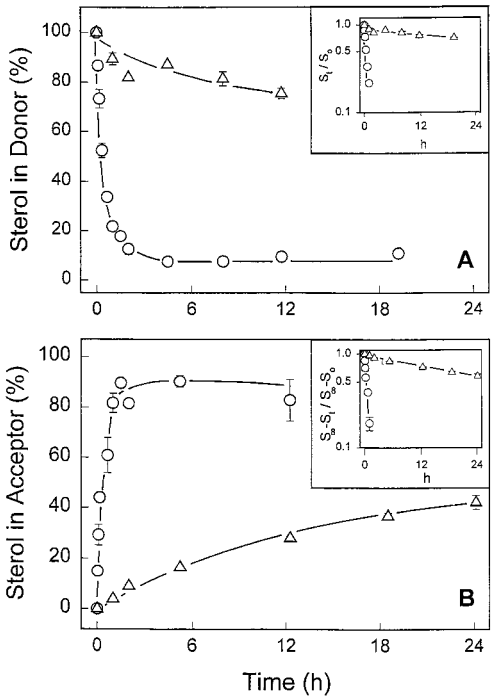

FIGURE 2: Time courses of spontaneous ChOOH and Ch transfer, as determined by departure from photoperoxidized ghosts (A) and uptake by SUVs (B) in the same reaction mixture. Loss of ChOOH (○) and Ch (△) from ghosts and acquisition by SUVs were monitored by HPTLC-PI. (Details about the reaction system are provided in the Figure 1 legend.) The inset in (A) shows a semilogarithmic plot of remaining analyte fraction vs time, where S_0 and S_t denote amount of sterol at zero time and time t, respectively. The inset in (B) shows a semilogarithmic plot representing analyte acquisition vs time, where S_0, S_t, and S_∞ denote zero time, time t, and infinite time, respectively. Means ± deviation of values from duplicate experiments are shown, one of which is represented in part in Figure 1. Apparent first-order transfer rate constants calculated from these data (±SD) are as follows: ChOOH, $(2.01 \pm 0.12) \times 10^{-2}$ min^{-1} (A), $(2.44 \pm 0.04) \times 10^{-2}$ min^{-1} (B); Ch, $(3.27 \pm 0.26) \times 10^{-4}$ min^{-1} (A), $(3.70 \pm 0.23) \times 10^{-4}$ min^{-1} (B).

SUV compartment because of its relatively large size (>6 times more membrane lipid than the donor compartment). We showed previously (*11*) that SUV-acquired ChOOH could be back-transferred to nonperoxidized ghosts, as expected if the process were freely reversible and capable of attaining equilibrium. That essentially all of the ChOOH in the reaction system was accounted for over at least a 12 h incubation period (Figure 2) further attests to the low reactivity of the system with respect to metal ion redox catalysis. A semilogarithmic plot representing sterol departure and sterol uptake kinetics is shown in the insets of Figure 2, respectively. As can be seen, the plots remain linear down to an ordinate value of at least 0.5, exhibiting apparent first-order rate constants for departure and acquisition that are nearly the same for either analyte (ChOOH, $k_d = 1.21$ h^{-1}, $k_a = 1.46$ h^{-1}; Ch, $k_d = 0.020$ h^{-1}, $k_a = 0.022$ h^{-1}). This similarity is consistent with the notion that spontaneous departure of either analyte was rate limiting, in agreement with previous evidence pertaining to Ch transfer (*2*, *35*). Thus, the rate constant for ChOOH transfer exceeded that for Ch transfer by ~65-fold under the conditions described. Knowing these constants and the initial sterol concentrations in ghost donors (see Figures 1 and 2), we calculated the initial transfer rates for ChOOH and Ch to be 159 and 62 nM/min, respectively.[2] Thus, even though the initial ChOOH con-

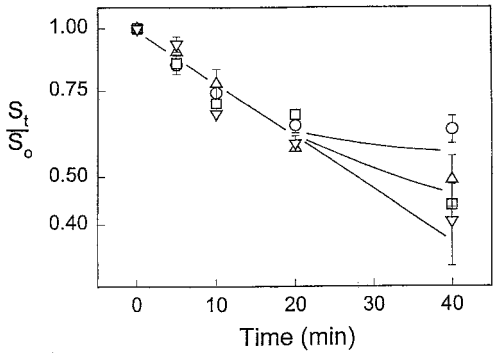

FIGURE 3: ChOOH transfer kinetics in relation to acceptor vs donor pool size. Reaction mixtures in PBS/DFO/10 μM BHT at 37 °C contained photoperoxidized DMPC/[^{14}C]Ch/DCP (50:40:1 by mol) SUVs (2.1 μM ChOOH; 0.06 mM SUV lipid) and ghost acceptors at the following lipid concentrations, 0.06 mM (○), 0.30 mM (□), 0.60 mM (△), and 0.90 mM (▽), giving ghost/SUV lipid mol ratios of 1:1, 5:1, 10:1, and 15:1, respectively. At the indicated times, SUV lipids were extracted and analyzed for remaining ChOOH by means of HPTLC-PI. ChOOH in the complete (SUV/ghost) system was determined alongside. Amount of lipid analyzed from the respective reaction mixtures: 1.2 nmol (SUV fraction); 3.0, 9.0, 16.5, and 24.0 nmol (SUV/ghost mixtures). Plotted data are means ± deviation of values from duplicate experiments. S_0 and S_t denote amount of ChOOH at zero time and time *t*, respectively.

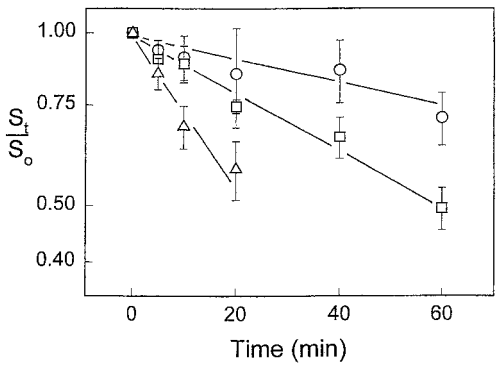

FIGURE 4: ChOOH transfer kinetics in relation to size of donor liposomes. Stock preparations of 50 nm (△), 100 nm (□), and 200 nm (○) DMPC/[^{14}C]Ch/DCP (50:40:1 by mol) vesicles were each photoperoxidized to a ChOOH level of 69 ± 4 μM. Reaction mixtures contained liposome donors (2.2 μM ChOOH, 0.06 mM liposomal lipid) and ghost acceptors (0.60 mM ghost lipid) in PBS/DFO/10 μM BHT at 37 °C. At the indicated incubation times, liposome and liposome/ghost samples were extracted and recovered lipid fractions analyzed for ChOOH by HPTLC-PI. Mean values from duplicate experiments are plotted. Apparent first-order rate constants calculated from the data (±SD) are as follows: (3.32 ± 0.42) × 10^{-2} min^{-1} (△); (1.10 ± 0.02) × 10^{-2} min^{-1} (□); (0.53 ± 0.10) × 10^{-2} min^{-1} (○).

centration in ghosts (~7 μM) was only ~4% of the original Ch concentration, the ChOOH transfer rate still exceeded the Ch rate by a substantial margin. We determined previously (*11*) that the ChOOH transfer rate increased linearly with ghost [ChOOH] over the 2−13 μM range.

Effect of Varying Acceptor/Donor Pool Ratio on ChOOH Transfer Kinetics. We asked whether changing the size of the acceptor pool relative to the donor pool would affect ChOOH transfer rate. These experiments were carried out using photoperoxidized SUVs as donors and nonoxidized ghosts as acceptors. As shown in Figure 3, the ChOOH level in SUVs incubated in the presence of ghosts at 1:1 lipid mol ratio decayed in an apparent first-order fashion out to ~20 min and leveled off after 40 min, presumably as the system reached equilibrium. There was no significant change in the decay kinetics upon increasing the ghost membrane concentration at a fixed SUV concentration. Thus, the apparent first-order rate constant and initial rate remained the same (~0.025 min^{-1} and ~53 nM/min, respectively) at lipid mol ratios of 1:1, 5:1, 10:1, and 15:1. Similar observations were made when the order of transfer was reversed, i.e., when ghosts delivered ChOOHs to a SUV pool of varying size (data not shown). These results, like those widely published for parent Ch (*1*, *2*), are consistent with those in Figure 2 and support a rate-limiting desorption/aqueous diffusion model for ChOOH transfer.

Effect of Varying Donor Vesicle Size on ChOOH Transfer Kinetics. Studies by other groups (*36*, *37*) have shown that unilamellar liposomes translocate Ch at rates that vary inversely with donor particle size, SUVs 25 nm in diameter, for example, releasing sterol substantially faster than those 80 nm in diameter (*36*). To learn whether ChOOH transfer from liposomal donors would exhibit similar size dependency, we photoperoxidized vesicles of average diameter 50, 100, and 200 nm to the same total ChOOH level and then compared rates of HPTLC-PI-assessed transfer to ghost acceptors in 10-fold lipid molar excess. As shown in Figure 4, the ChOOH transfer rate increased progressively with decreasing vesicle diameter, 50 nm SUVs releasing peroxide 3 times and 6.3 times faster than 100 and 200 nm LUVs, respectively. The initial ChOOH composition of these liposome preparations was essentially the same [45 ± 3% 7α/7β-OOH; 28 ± 3% 5α-OOH; 27 ± 4% 6α/6β-OOH (mean ± SEM)], ruling out any size-related compositional differences (see below) as a possible explanation for these findings. Whereas peroxide transfer rates were strongly influenced by donor vesicle size, acceptor vesicle size proved to be relatively unimportant in this regard (*11*), in agreement with Ch transfer findings (*37*). As proposed by others for Ch (*2*, *36*, *37*), we attribute our findings to differences in lipid packing/interaction in the membrane bilayer, relatively loose interaction in highly curved SUVs making ChOOH desorption more favorable than in larger vesicles.

Ionic Strength Effects on Transfer Kinetics. Increasing the ionic strength of the aqueous compartment is known to slow the intermembrane transfer/exchange of Ch (*38*, *39*). We asked whether ChOOH transfer would be similarly altered by ionic strength and, if so, how the magnitude of this effect would compare with that observed for Ch transfer. Sterol movement from photoperoxidized SUVs to ghosts was measured at several different ionic strength levels, ranging from 0.02 to 0.46 M. As shown in Table 1, the rate constants for both Ch and ChOOH transfer decreased steadily over the indicated range. However, the extent of change was different for the two sterols, k_{Ch} decreasing by 49% on going from 0.02 to 0.46 M ionic strength but k_{ChOOH} decreasing by only 24%. Therefore, ChOOHs as a group were substantially less sensitive to ionic strength, presumably because of their greater polarity and aqueous solubility compared with parent Ch.

[2] Initial rates were also determined by direct measurement of sterol uptake over a relatively short period, 5 min in the case of ChOOH. Although similar values could be obtained by this approach, at least for ChOOH (*11*), determination via rate constant is considered to be more accurate.

Table 1: Transfer Rate Constants for Ch and ChOOH in Relation to Ionic Strength of the Aqueous Medium[a]

ionic strength (M)	Ch k ($\times 10^2$ h^{-1})[b]	ChOOH k (h^{-1})[b]
0.020	5.71 ± 0.09	2.04 ± 0.08
0.039	5.52 ± 0.08	1.92 ± 0.20
0.11	5.40 ± 0.06	1.75 ± 0.11
0.19[c]	4.63 ± 0.07	1.62 ± 0.10
0.46	2.91 ± 0.06	1.56± 0.19

[a] ChOOH and Ch transfer from SUVs to ghosts was monitored. Each reaction system contained photoperoxidized DMPC/[^{14}C]Ch/DCP SUVs (5:4:0.1 by mol; 60 μM total lipid) and nonoxidized ghosts (600 μM total lipid). Starting concentrations of SUV [^{14}C]Ch and [^{14}C]ChOOH were 26.5 and 2.5 μM, respectively. Except where noted, the aqueous medium contained only 0.1 mM DFO and NaH_2PO_4/Na_2HPO_4 at varying concentrations to give the indicated ionic strengths at pH 7.4 ± 0.1. Transfer incubations were carried out at 37 °C, and extracts from SUV samples were analyzed by HPTLC-PI. [b] Apparent first-order rate constants were determined from the decay kinetics of each SUV-associated analyte; values are means ± SD. [c] The aqueous medium in this case consisted of PBS + 0.1 mM DFO.

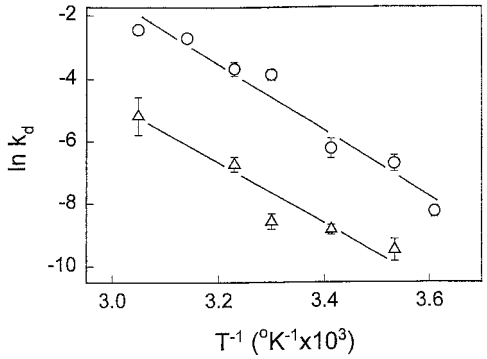

FIGURE 5: Arrhenius plot for ChOOH and Ch transfer from ghost membranes to liposomal membranes between 4 and 55 °C. Reaction mixtures consisting of photoperoxidized [^{14}C]Ch-labeled ghosts and SUV acceptors were as described in Figure 1. Transfer incubations were carried out in a thermostated water bath maintained at various temperatures (±0.1 °C) over the indicated range. At various time points for each temperature, ghosts were pelleted, washed, and extracted; lipid fractions were analyzed for remaining Ch and ChOOH, using HPTLC-PI. The apparent first-order rate constants were determined for each analyte class and plotted against reciprocal absolute temperature, as shown: ChOOH (○); Ch (△). Plotted points are means ± deviation of values from duplicate experiments. The data for each analyte were fitted to a straight line by linear regression (r = 0.96 and 0.92 for ChOOH and Ch, respectively). Activation energies (kJ/mol) calculated from the line slopes are as follows (±SD): 84.7 ± 3.4 for ChOOH; 78.6 ± 3.5 for Ch.

Activation Energy for ChOOH vs Ch Transfer. The large differences in the transfer rate constants for Ch and aggregate ChOOH (Figure 2) prompted us to assess whether their transfer activation energies were also different. We examined this by monitoring sterol transfer from ghosts to SUVs as a function of temperature over the 4−55 °C range. Under the metal ion-depleted/inactivated conditions used, the ChOOH concentration in the complete system decreased by <8% over a 1 h measurement period at the highest temperature used, indicating that peroxide instability or de novo generation during transfer was not a significant problem. Ch loss over a 24−36 h measurement period was also small (<5%). Figure 5 shows Arrhenius plots of ln k_d vs 1/T for ChOOH and Ch, k_d representing the rate constant for sterol deprature from ghosts and T the absolute temperature. Both plots are linear over the temperature range examined, the calculated activation energy for ChOOH being 85 ± 3 kJ/mol and that for Ch being 79 ± 4 kJ/mol. Reverse transfer, i.e., from SUVs to ghosts, gave essentially the same values (data not shown), which are similar to those reported previously for Ch transfer in a variety of donor/acceptor membrane systems (*35*, *40*). The insignificant (~7%) difference between the ChOOH and Ch activation energies indicates that even though the rate constant for ChOOH desorption exceeded that for Ch desorption by >60-fold (cf. Figure 2), the net energy required for separation from the membrane surface was essentially the same.

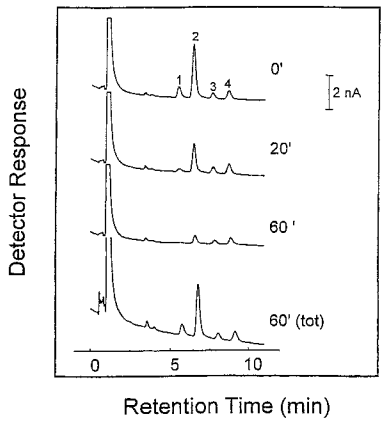

FIGURE 6: HPLC-EC(Hg) profiles depicting progressive transfer of individual ChOOH species from ghost membranes to liposomal membranes. The reaction system was similar to that described in Figures 1 and 2, except that the ghost Ch was not ^{14}C-labeled in this case. Total [ChOOH] at the outset was 13.7 μM in bulk suspension. At each of the indicated times (0−60 min), samples from the incubation mixture were centrifuged; the ghost pellets were washed twice with cold PBS and extracted. Recovered lipids were analyzed by HPLC-EC(Hg) (~3.1 nmol of total lipid per injection). A noncentrifuged sample representing total ChOOH in the reaction mixture at 60 min (60′ tot) was extracted and analyzed alongside (~11.6 nmol of ghost + SUV lipid per injection). Peak assignments for ChOOH isomers are as follows: (1) 7α/7β-OOH (5.7 min); (2) 5α-OOH (6.7 min); (3) 6α-OOH (8.0 min); (4) 6β-OOH (9.1 min). Detector sensitivity was 5 nA full scale for all scans.

Transfer Kinetics for Individual ChOOH Species. HPTLC-PI analysis allowed us to distinguish the transfer kinetics of Ch and overall ChOOH but not the kinetics of different positional isomers comprising the photogenerated ChOOH population, viz., 5α-OOH, 6α-OOH, 6β-OOH, 7α-OOH, and 7β-OOH (*31*, *41*). 5α-OOH, 6α-OOH, and 6β-OOH are singlet oxygen adducts (*42*), whereas 7α- and 7β-OOH derive either from 5α-OOH rearrangement or from free radical reactions (*33*, *43*). To monitor the transfer properties of these species, we used a reverse-phase liquid chromatographic technique developed in this laboratory, HPLC-EC(Hg), which resolves all of these species from one another except 7α-OOH from 7β-OOH. HPLC-EC(Hg) profiles from a ghost donor/SUV acceptor experiment are shown in Figure 6. One sees that transfer incubation resulted in a progressive loss of donor 7α/7β-OOH, 5α-OOH, 6α-OOH, and 6β-OOH over a 1 h period. (These species comprised 10%, 67%, 6%, and 17%, respectively, of total ChOOH in this particular experiment.) Analysis of the complete system (Figure 6, bottom trace) indicated that there was no net loss of any of these peroxides, all of which accumulated reciprocally in the SUV compartment (results not shown). First-order plots depicting the decay kinetics of individual ChOOHs (cf. Figure 6) are

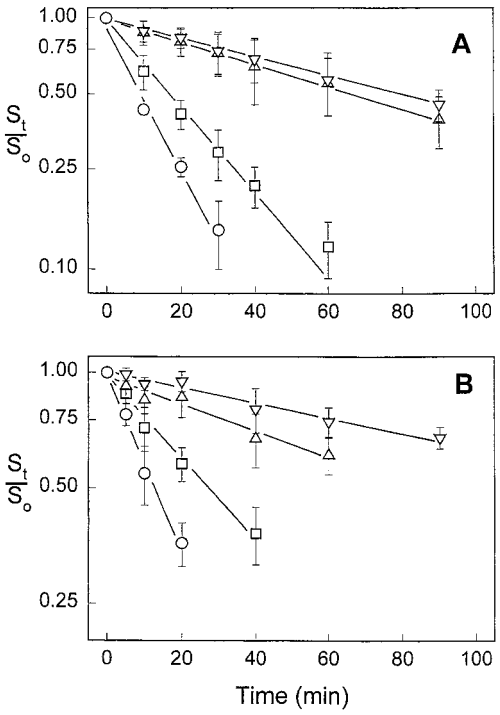

FIGURE 7: First-order kinetic plots for the intermembrane transfer of individual ChOOH species, as monitored by HPLC-EC(Hg). (A) Transfer from photoperoxidized ghost membranes to SUVs; experimental conditions were as described in Figure 6. Initial concentrations of ghost hydroperoxides in bulk suspension were as follows: 7α/7β-OOH (○, 1.4 μM); 5α-OOH (□, 9.2 μM); 6α-OOH (△, 0.8 μM); 6β-OOH (▽, 2.3 μM). Data points are means ± SD of values from four separate experiments. (B) Transfer from photoperoxidized SUVs to ghost membranes. Reaction mixtures contained ghosts at 0.39 mM total lipid and peroxidized DMPC/Ch/DCP (5:4:0.1 by mol) SUVs at 3.4 μM total ChOOH and 60 μM total SUV lipid. Other details were as described in Figure 4. ChOOH loss from SUVs over time was monitored by HPLC-EC-(Hg). Initial concentrations of SUV hydroperoxides were as follows: 7α/7β-OOH (○, 1.7 μM); 5α-OOH (□, 0.74 μM); 6α-OOH (△, 0.34 μM); 6β-OOH (▽, 0.58 μM). Data points are means ± SD of values from six separate experiments.

shown in Figure 7A. The plots are linear down to at least 20% residual peroxide and then curve off, suggesting approach to an acceptor-favored equilibrium state (cf. Figure 2). Significant differences are observed in the departure kinetics of the various ChOOHs, the apparent first-order rate constant for 7α/7β-OOH being approximately twice that of 5α-OOH and 7 times that of 6β-OOH (Table 2, system 1). It is important to note that the rank order of these rate constants (7α/7β-OOH > 5α-OOH > 6α-OOH > 6β-OOH) is the inverse of that relating to the reverse-phase HPLC retention times of the different species (Figure 6). Thus, 7α/7β-OOH with the shortest retention time (least hydrophobicity) translocated most rapidly, whereas 6β-OOH with the longest retention time (greatest hydrophobicity) translocated least rapidly. A plausible explanation, similar to that applied to Ch vs phospholipid transfer/exchange (*2*, *35*), is that the ChOOH desorption rate increased with increasing hydrophilicity, resulting in proportionately more peroxide in the aqueous transit pool. Calculation of initial ChOOH transfer rates for the ghost donor/SUV acceptor experiment, knowing starting concentrations in donor membranes (Figure 7A) and the average rate constants (Table 2, system 1), gave the following values: 101 nM/min (7α/7β-OOH); 376 nM/min (5α-OOH); 10 nM/min (6α-OOH); 24 nM/min (6β-OOH). Ghost membranes accumulate 5α-OOH much faster than 6α-OOH or 6β-OOH during singlet oxygen-mediated photooxidation, with relatively little rearrangement of 5α-OOH to 7α-OOH (*28*). This accounts for the relatively high concentration of donor 5α-OOH in the Figure 6 experiment and the high initial transfer rate for this peroxide (11 times that of 6α- and 6β-OOH combined and nearly 4 times that of 7α/7β-OOH).

Table 2: Transfer Rate Constants for Individual ChOOH Species

transfer system[a]	k (h^{-1})[b]			
	7α/7β-OOH	5α-OOH	6α-OOH	6β-OOH
1. ghost → SUV	4.62 ± 0.31 4.06 ± 0.18[c]	2.24 ± 0.19 2.67 ± 0.19[c]	0.65 ± 0.14 0.79 ± 0.15[c]	0.55 ± 0.10 0.68 ± 0.08[c]
2. SUV → ghost	3.38 ± 0.58	2.03 ± 0.43	0.48 ± 0.14	0.34 ± 0.06
3. SUV → cell	0.191 ± 0.019[d]	0.096 ± 0.020	na[e]	0.026 ± 0.001

[a] System 1, same as described in Figure 7A; system 2, same as described in Figure 7B; system 3, same as described in Figure 8A. [b] Apparent first-order rate constants for ChOOH transfer. Values are means ± SD, based on at least four time points from four experiments (system 1), six experiments (system 2), and two experiments (system 3). Except where noted, values were calculated from decay (departure) plots. [c] Rate constants calculated from plots (not shown) of ChOOH uptake by SUVs in system 1. [d] Only 7α-OOH initially in this case. [e] na = not applicable.

The results of a reciprocal experiment involving photoperoxidized SUV donors and ghost acceptors indicated a similar trend of kinetic differences among the ChOOH species, 7α/7β-OOH having the highest rate constant and 6β-OOH the lowest (Table 2, system 2). The rate constant values in this case appeared to be ~30% lower on average than those determined for system 1 (Table 2). This difference might be explained by the nature of the donor phospholipid, saturated lipids (as in our SUVs) disfavoring transfer and highly unsaturated lipids (as in ghosts) favoring it (*2*). We found previously (*29*) that the relative amounts of 5α-OOH and 7α/7β-OOH that accumulate during photooxidation also depend on the degree of phospholipid unsaturation. Thus, in DMPC LUVs 5α-OOH rapidly isomerizes to 7α-OOH after reaching a 7−8% yield, whereas POPC LUVs and ghost membranes are progressively less susceptible to this (*29*). The relatively high 7αβ-OOH/5α-OOH ratio in the Figure 7B experiment, where the overall ChOOH yield was ~13%, can be explained on this basis. Initial rate calculations for this arrangement (Figure 7B; Table 2, system 2) indicated that 7α/7β-OOH translocated ~4 times faster than 5α-OOH and ~16 times faster than 6α- and 6β-OOH combined. Thus, host membrane lipid composition can play a crucial role in determining whether 5α-OOH or 7α/7β-OOH translocates faster in any given system.

Transfer-Dependent Cytotoxicity of Different ChOOH Species. Having demonstrated different transfer kinetics for 5α-OOH, 6α-OOH, 6β-OOH, and 7α/7β-OOH, we asked whether this might manifest itself in terms of different degrees of cytotoxicity. To examine this, we used COH-BR1 cells, a breast tumor line reported to be deficient in the selenoperoxidase GPX4 (*22*). GPX4, also known as PHGPX (*23*), can catalyze the two-electron reduction of phospholipid- and cholesterol-derived hydroperoxides in membranes (*44*) and thus may play a crucial role in cellular defense against

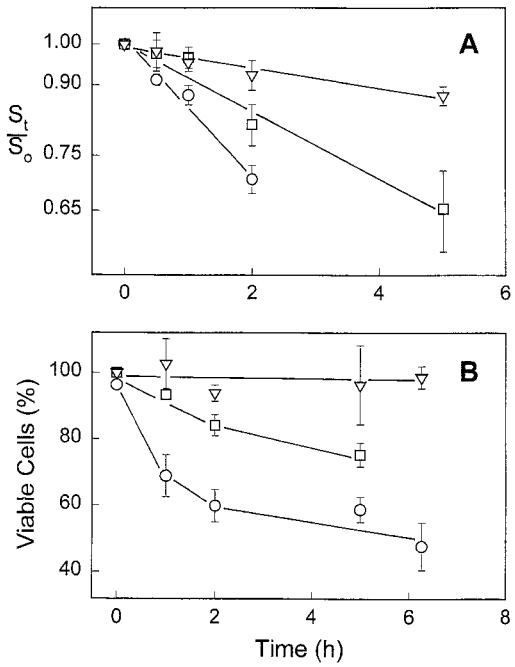

FIGURE 8: Transfer-dependent cytotoxicity of different ChOOH species. Near-confluent COH-BR1 cells in six-well plates were overlaid with POPC/Ch/ChOOH (10:7:1 by mol) SUVs in PBS supplemented with D-glucose, $CaCl_2$, and $MgCl_2$. The cell/SUV lipid ratio was ~0.8:1 (mol/mol), and ChOOH was either 7α-OOH, 5α-OOH, or 6β-OOH at an initial concentration of 5.6 μM (see Materials and Methods for additional details). At the indicated times during incubation at 37 °C, the SUV-containing medium was removed and extracted; recovered ChOOHs in lipid fractions were subsequently determined by HPLC-EC(Hg) analysis. Immediately after SUV removal, the cells were detached by trypsinization and viability was assessed by trypan blue exclusion assay. (A) First-order plots comparing the transfer uptake of the different ChOOHs by cells. (B) Corresponding viability losses induced by the different ChOOHs. Data points are means ± deviation of values from duplicate experiments: 7α-OOH (○); 5α-OOH (□); 6β-OOH (▽).

peroxidative stress (*45*). At present, no other enzyme is known to be capable of reducing/detoxifying ChOOHs. Using a highly sensitive/specific HPLC-EC(Hg) assay based on 7α-OOH reduction (*14*), we have recently shown that COH-BR1 cells express <5% of the GPX4 specific activity of two other mammalian lines grown under the same conditions (*46*). The lack (or severe deficiency) of GPX4 in COH-BR1 cells made them ideal for evaluating transfer-limited cytotoxicity per se, i.e., without the complications of differential ChOOH detoxification (*13*). Near-confluent cells were exposed to three different preparations of POPC/Ch/ChOOH (10:7:1 by mol) SUVs, where ChOOH (either 5α-OOH, 6β-OOH, or 7α-OOH) was incorporated at fabrication rather than via photooxidation. Transfer incubation was carried out in PBS supplemented with Mg^{2+}, Ca^{2+}, and D-glucose. All ChOOHs were found to be sufficiently stable during transit in this medium, and control cells underwent no more than ~15% inactivation over a 6 h period. As shown in Figure 8A, each of the three SUV ChOOHs decayed exponentially during transfer incubation with cells, the overall kinetic trend being similar to that observed with the SUV/ghost systems (Figure 7), i.e., 7α-OOH > 5α-OOH > 6β-OOH. The apparent first-order rate constant calculated for each ChOOH species from these data (Table 2, system 3) is ~25 times lower than that determined for the ghost/SUV system (Table 2; system 1). The reason for this is not clear, but it might be ascribed to limitations of the acceptor pool, including relatively small size and nonaccessibility of the attached cell surface. A decrease in the viable cell count was observed during 6 h of transfer incubation, the initial rate of which correlated with the ChOOH transfer rate (Figure 8B). Thus, 7α-OOH, 5α-OOH, and 6β-OOH killed ~40%, ~15%, and <10% of the cells, respectively, over a 2 h period. The slowdown in 7α-OOH-induced killing after 2 h (Figure 8B) may reflect the fact that this system was nearing transfer equilibrium at that time. Cytolethality was effectively abolished when ChOOH transfer was carried out in the presence of 100 μM DFO (results not shown), indicating that iron-catalyzed free radical reactions were responsible (*33*, *45*).

DISCUSSION

We recently reported the first kinetic evidence for rapid and spontaneous intermembrane translocation of a family of photochemically generated ChOOHs (*11*). Earlier work (*17*) had established that one particular ChOOH, 5α-OOH, could translocate from liposomes to erythrocyte ghosts, thus sensitizing the latter to chain peroxidative damage. However, the kinetics of the translocation process were not examined in that work. We have now confirmed and extended our recent findings (*11*), showing not only that the rate constant for ChOOH transfer far exceeds that of parent Ch but that the various molecular species in the ChOOH population differ significantly in their transfer kinetics. We refer to this process as "transfer" rather than "exchange" because it is not clear whether a ChOOH molecule (initially present only in the donor compartment) might exchange for Ch or some other species in the acceptor compartment. When a large SUV sink was used, ChOOH decay on a first-order plot remained linear to at least 20% of its initial value (Figure 2), implying that a single kinetic pool of ChOOH existed in the ghost donor. Thus, there was no obvious difference between ChOOH emanating from the inner vs the outer membrane leaflet. This was not unexpected, however, because ghost membranes contain at least one large lytic fissure (*47*), which would presumably allow equilibration of endofacial and exofacial hydroperoxides. On the other hand, previous studies involving closed liposomal donors (*35*) have established that Ch exchanges with a single rate constant, whereas phosphatidylcholine shows mixed kinetics due to relatively slow transfacial movement.

For most of our experiments, ChOOHs were generated de novo in donor membranes by dye-sensitized (singlet oxygen-mediated) photooxidation (*41*). An advantage of this approach is that LOOHs typically accumulate linearly with light dose, so that yields can be predetermined with great accuracy. The initial rate of intermembrane ChOOH transfer was found to be zero order with respect to acceptor concentration as the acceptor/donor lipid ratio was increased from 1:1 to 15:1. Accordingly, this process, like Ch transfer (*2*), conforms to an aqueous diffusion mechanism in which desorption from the donor membrane is rate limiting. As demonstrated previously for Ch (*36*, *37*), the rate of overall ChOOH transfer at a fixed peroxide pressure increased with decreasing donor size, consistent with the idea that departure is facilitated by decreasing the lipid packing density in the donor membrane outer leaflet. Consequently, in a biological setting, small donors could potentially be more dangerous

to vulnerable acceptors than larger donors. Our preliminary findings with peroxidized liposomes and cell targets (A. Vila and A. W. Girotti, unpublished data) lend support to this idea. Most of the experiments in this study were carried out at a single concentration of donor ChOOH, typically between 2 and 10 μM in bulk suspension. We showed previously (*11*) that the initial rate of ChOOH desorption from ghost membranes increased linearly with concentration over the 2−13 μM range; thus, the rate constant remains unchanged over this range. Whether going to still higher concentrations would result in any disproportionate changes in rate constant (possibly because of more extensive perturbation of the bilayer) remains to be investigated. It seems reasonable to predict that, in progressively more peroxidized donor membranes, desorption rate will increase with ChOOH concentration but that structural changes, e.g., looser lipid packing, will also play a role.

The activation energies for Ch and collective ChOOH departure from peroxidized ghosts were found to be essentially the same, viz., ~85 kJ/mol, which falls within the range of published values for Ch (*2*, *35*). Approximately the same value was obtained for individual ChOOHs (data not shown) or when departure from peroxidized DMPC/Ch/DCP SUVs was measured. Thus, desorption energetics appeared to be invariant with donor membrane composition, at least in the systems examined. Intuitively, one might expect the activation energy for ChOOH transfer to be lower than that for Ch transfer because the former is more polar (Figure 2). Therefore, observing the same value for both analytes was initially surprising. However, there is a reasonable explanation if one considers the overall structural similarities between the ChOOHs studied and parent Ch. Since the A/B-ring hydroperoxyl group of 5α-OOH and the other ChOOHs is not too distant from the A-ring hydroxyl group, these molecules, though more polar than Ch itself, retain most of its amphiphilic character, with the same hydrophobic "tail" portion and a relatively rigid hydrophilic "head" portion. On this basis, one might expect ChOOH and Ch to have similar free energy requirements for transfer activation and desorption, where activation refers to movement of the intercalated hydrophobic portion of the molecule to the bilayer−water interface (*48*). On the other hand, ChOOH released into the aqueous phase would bring the system to a lower free energy state than Ch release, based on hydrophobic effect considerations (*49*), and this would translate into a greater off-rate for ChOOH, as observed. It would be of interest to determine how the activation energy of 25-hydroperoxycholesterol (25-OOH) (*50*) compares with that of the A/B-ring hydroperoxides studied in this work. Since 25-OOH has opposing polar groups, its bilayer interaction is expected to be quite weak compared with 5α-OOH, for example, and this may be reflected in a lower activation energy for 25-OOH. Whereas 25-OOH transfer has not been assessed, 25-OH (the diol analogue) has been shown to translocate much more rapidly than Ch (*7*).

In addition to showing that ChOOHs as a whole transfer faster than Ch, we found that the four resolvable isomers in the ChOOH population exhibit significantly different transfer kinetics, with rate constants decreasing in the following order: 7α/7β-OOH > 5α-OOH > 6α-OOH > 6β-OOH. Reverse-phase HPLC retention times of these isomers increased in the same order, showing that there was a direct correlation between increasing hydrophilicity and faster transfer. A similar correlation has been observed for various nonoxidized phospholipids with different fatty acyl chain lengths (*48*, *51*). While these are the first reported transfer measurements for nonesterified ChOOH species, at least two other groups (*6*, *7*) have compared the transfer kinetics of relativley stable oxides such as 7α-hydroxycholesterol (7α-OH), 7β-hydroxycholesterol (7β-OH), 7-ketocholesterol (7-one), and 25-hydroxycholesterol (25-OH). Being more polar than Ch, all of these species translocated more rapidly between liposomal membranes than the parent sterol. However, there appeared to be no direct correlation between desorption rate from donor vesicles and hydrophilicity, as determined by retention time on a reverse-phase HPLC column (*6*). For example, 7-keto, 7α-OH, and 7β-OH differed greatly in their relative transfer rates (1.0, 2.3, and 11.6, respectively) but little (<25%) in hydrophilicity. It was concluded that faster transfer of these more polar sterols results from weaker interactions with surrounding phospholipids (looser packing) rather than increased solubility in the aqueous compartment. It is not obvious why the hydrophilicity/transfer rate relationship we observed for ChOOHs did not apply for the nonperoxy oxysterols (*6*). However, one possiblity may relate to the fact that these compounds were used at much higher levels in donor liposomes than the ChOOHs in our study (25 mol % vs 3−5 mol %). The higher levels may have had a greater, yet varied, membrane-perturbing effect, tending to make this more important than hydrophilicity as a determinant of transfer rate. Whether this might apply at high ChOOH densities remains to be seen.

Using COH-BR1 cells as acceptors, we showed that ChOOH transfer could have cytotoxic consequences. Moreover, we found that the time-dependent degree of cytotoxicity for three different ChOOHs decreased in parallel with their rates of transfer uptake as follows: 7α-OOH > 5α-OOH > 6β-OOH. COH-BR1 cells were well suited for this experiment, since they express little, if any, GPX4 and are thus practically defenseless against ChOOHs (*22*). By way of contrast, we showed previously (*13*, *41*) that L1210 leukemia cells, which exhibit at least 40 times the GPX4 activity of COH-BR1 cells under the same selenium supplementation (*46*), were substantially more resistant to a ChOOH challenge (*13*, *41*). When individual ChOOHs were delivered to L1210 cells at the same rate (i.e., at a very large donor/acceptor ratio), their toxic potencies varied as follows: 5α-OOH ≫ 7α-OOH > 6β-OOH (*13*). In this earlier work, we also examined the action of purified GPX4 or GPX4 in L1210 lysates on individual ChOOHs, finding that the rate constants for peroxide decay at a given enzyme level decreased in the following order: 6β-OOH > 7α-OOH ≫ 5α-OOH (*13*). Thus, 5α-OOH, the poorest GPX4 substrate, was the most cytotoxic of the ChOOHs studied, whereas 6β-OOH, the best substrate, was the least cytotoxic. We reasoned from these findings that once ChOOHs are taken up by cells, their relative toxicities vary inversely with susceptibility to GPX4-mediated detoxification. In the case of GPX4-deficient COH-BR1 cells (Figure 8), cytotoxicity was found to be transfer limited at an acceptor/donor lipid ratio near unity. (With cell monolayers it was difficult to attain higher ratios while maintaining a realistically low peroxide titer in the donor compartment.) On the basis of the results with L1210 cells (see above; *13*), one can predict that using a high donor/

acceptor ratio with COH-BR1 cells would tend to equalize 5α-OOH, 6*β*-OOH, and 7α-OOH cytotoxicity. This would follow from our previous findings that these peroxides undergo iron-catalyzed one-electron reduction at essentially the same intrinsic rate (*33*). One-electron reduction could trigger free radical-mediated (chain) peroxidation reactions which damage and perturb acceptor membranes. Along these lines, we showed recently (*11*) that [^{14}C]Ch-labeled SUVs containing transfer-acquired ChOOHs accumulate characteristic free radical oxidation products of Ch when exposed to an electron donor (ascorbate) and lipophilic iron. One can infer from this that peroxidative chain reactions induced by one-electron turnover of translocated ChOOHs also played an important role in COH-BR1 cell killing (Figure 8B).

These and previous findings (*11*) are consistent with the idea that ChOOH transfer, both intracellular and extracellular, can occur under physiological conditions. Similar considerations apply to other LOOH classes, e.g., phospholipid hydroperoxides, although these have not yet been studied as extensively as ChOOHs. Intracellularly, LOOHs might move from mitochondria (which are under relatively high oxidative pressure) to the nucleus, where DNA could be damaged. Conversely, there might be situations in which LOOH transfer has cytoprotective implications, i.e., relocation to sites at which enzymatic or nonenzymatic antioxidants are more available. Several types of extracellular LOOH trafficking are also possible: (i) between cells (e.g., red cells, neutrophils, endothelial cells), (ii) between low-density and high-density lipoproteins (LDL, HDL), and (iii) between cells and lipoproteins. It is well-known that the presence of LOOHs in LDL can predispose it to free radical-mediated oxidative modification (*52*, *53*). Such oxidation can enhance LDL uptake by the vascular wall and is linked to atherogenesis (*54*). The source of "preexisting" ChOOHs and other LOOHs in LDL has been under much debate (*55*). While spontaneous or protein-facilitated transfer from cell membranes (e.g., red cell or activated phagocyte membranes) has been considered (*53*, *55*, *56*), there has been little direct evidence for this. On the other hand, transfer/exchange of cholesteryl ester hydroperoxides (CEOOHs), both between LDL and HDL and between HDL and liver cells, has been well documented (*57*−*59*). In one of these studies (*59*), CEOOH transfer from LDL to HDL was found to be strongly enhanced by a cholesteryl ester transfer protein. Along similar lines, we have recently determined that sterol transfer protein-2 purified from beef liver (*60*) markedly stimulates ghost/SUV ChOOH transfer (A. Vila and A. W. Girotti, unpublished observation).

Although this study impacts on all types of oxidative stress that produce ChOOHs and other LOOHs, it has special meaning in the area of singlet oxygen-mediated peroxidative stress, e.g., that induced by photodynamic action. 5α-OOH translocation can be highlighted in this regard. In a cell under singlet oxygen challenge, e.g., a skin fibroblast exposed to ultraviolet-A radiation (*61*), 5α-OOH would be generated much more rapidly than other ChOOHs (*41*) but detoxified very slowly by the GSH/GPX4 system (*13*). Intermembrane transfer of 5α-OOH would be favored under these circumstances, and this could greatly expand its range of activity as a toxic oxidant. Such possibilities for 5α-OOH, and to varying degrees other LOOHs, have not been well recognized up to now.

ACKNOWLEDGMENT

We appreciate Tamas Kriska's assistance in the cellular aspects of this study. Helpful discussions with Karol Subczynski regarding ChOOH transfer activation are also gratefully acknowledged.

REFERENCES

1. Dawidowicz, E. A. (1987) in *Current Topics in Membranes and Transport* (Klausner, R. D., Kempf, C., and van Renswoude, J., Eds.) Vol. 29, pp 175−202, Academic Press, New York.
2. Phillips, M. C., Johnson, W. J., and Rothblat, G. H. (1987) *Biochim. Biophys. Acta 906*, 223−276.
3. Brown, R. E. (1992) *Biochim. Biophys. Acta 1113*, 375−389.
4. Liscum, L., and Munn, N. J. (1999) *Biochim. Biophys. Acta 1438*, 19−37.
5. Kan, C.-C., and Bittman, R. (1991) *J. Am. Chem. Soc. 113*, 6650−6656.
6. Kan, C.-C., Yan, J., and Bittman, R. (1992) *Biochemistry 31*, 1866−1874.
7. Van Amerongen, A., Demel, R. A., Westerman, J., and Wirtz, K. W. A. (1989) *Biochim. Biophys. Acta 1004*, 36−43.
8. Girotti, A. W. (1985) Mechanisms of lipid peroxidation, *J. Free Radicals Biol. Med. 1*, 87−95.
9. Porter, N. A., Caldwell, S. E., and Mills, K. A. (1995) *Lipids 30*, 277−290.
10. Girotti, A. W. (1998) *J. Lipid Res. 39*, 1529−1542.
11. Vila, A., Korytowski, W., and Girotti, A. W. (2000) *Arch. Biochem. Biophys. 380*, 208−218.
12. Korytowski, W., Bachowski, G. J., and Girotti, A. W. (1991) *Anal. Biochem. 197*, 149−156.
13. Korytowski, W., Geiger, P. G., and Girotti, A. W. (1996) *Biochemistry 35*, 8670−8679.
14. Korytowski, W., Geiger, P. G., and Girotti, A. W. (1999) *Methods Enzymol. 300*, 23−33.
15. Bloch, K. (1983) *Crit. Rev. Biochem. 13*, 47−92.
16. Buettner, G. R. (1988) *J. Biochem. Biophys. Methods 16*, 27−40.
17. Geiger, P. G., Korytowski, W., and Girotti, A. W. (1995) *Photochem. Photobiol. 62*, 580−587.
18. Fairbanks, G., Steck, T. L., and Wallach, D. F. H. (1971) *Biochemistry 10*, 2606−2616.
19. Lowry, O. H., Rosebrough, N. L., Farr, A. L., and Randall, R. J. (1951) *J. Biol. Chem. 193*, 265−275.
20. Van Deenen, L. L. M., and De Gier, J. (1974) in *The Red Blood Cell* (Surgenor, D. M., Ed.) Vol. 1, pp 147−161, Academic Press, New York.
21. Zhao, Y., and Marcel, Y. L. (1990) *Biochemistry 35*, 7141−7180.
22. Esworthy, R. S., Baker, M. A., and Chu, F.-F. (1995) *Cancer Res. 55*, 957−962.
23. Maiorino, M., Chu, F.-F, Ursini, F., Davies, K. J. A., Doroshow, J. H., and Esworthy, R. S. (1991) *J. Biol. Chem. 266*, 7728−7732.
24. Bradford, M. M. (1976) *Anal. Biochem. 72*, 248−254.
25. Burns, C. P., Wei, S. L., Welshman, I. R., Wiebe, D. A., and Spector, A. A. (1977) *Cancer Res. 37*, 1991−1997.
26. Lin, F., Geiger, P. G., and Girotti, A. W. (1992) *Cancer Res. 52*, 5282−5290.
27. Paquette, B., Ali, H., Langois, R., and van Lier, J. E. (1988) *Photochem. Photobiol. 47*, 215−220.
28. Beckwith, A. L. J., Davies, A. G., Davison, I. G. E., Maccoll, A., and Mruzak, M. H. (1989) *J. Chem. Soc., Perkin Trans. 2*, 815−824.
29. Korytowski, W., Bachowski, G. J., and Girotti, A. W. (1992) *Photochem. Photobiol. 56*, 1−8.
30. Korytowski, W., Geiger, P. G., and Girotti, A. W. (1995) *J. Chromatogr. B 670*, 189−197.
31. Girotti, A. W., and Korytowski, W. (2000) *Methods Enzymol. 319*, 85−100.

32. Phillips, H. J. (1973) in *Tissue Culture* (Kruse, P. F., Jr., and Patterson, M. K., Eds.) pp 406−408, Academic Press, New York.
33. Korytowski, W., Wrona, M., and Girotti, A. W. (1999) *Anal. Biochem. 270*, 123−132.
34. Johnston, R. F., Pickett, S. C., and Barker, D. L. (1990) *Electrophoresis 11*, 355−360.
35. McLean, L. R., and Phillips, M. C. (1981) *Biochemistry 20*, 2893−2900.
36. McLean, L. R., and Phillips, M. C. (1984) *Biochim. Biophys. Acta 776*, 21−26.
37. Fugler, L., Clejan, S., and Bittman, R. (1985) *J. Biol. Chem. 260*, 4098−4102.
38. Hapala, I., Butko, P., and Schroeder, F. (1990) *Chem. Phys. Lipids 56*, 37−47.
39. Li, Q.-T., and Sawyer, W. H. (1992) *Chem. Phys. Lipids 63*, 55−63.
40. McLean, L. R., and Phillips, M. C. (1982) *Biochemistry 21*, 4053−4059.
41. Korytowski, W., and Girotti, A. W. (1999) *Photochem. Photobiol. 70*, 484−489.
42. Kulig, M. J., and Smith, L. L. (1973) *J. Org. Chem. 38*, 3639−3642.
43. Smith, L. L., Teng, J. I., Kulig, M. J., and Hill, F. L. (1973) *J. Org. Chem. 38*, 1763−1765.
44. Thomas, J. P., Geiger, P. G., Maiorino, M., Ursini, F., and Girotti, A. W. (1990) *J. Biol. Chem. 265*, 454−461.
45. Girotti, A. W. (1998) *J. Lipid Res. 39*, 1529−1542.
46. Hurst, R., Korytowski, W., Kriska, T., Esworthy, R. S., Chu, F.-F., and Girotti, A. W. (2001) *Free Radical Biol. Med. 31*, 1051−1065.
47. Lieber, M. R., and Steck, T. L. (1982) *J. Biol. Chem. 257*, 11651−11659.
48. McLean, L. R., and Phillips, M. C. (1984) *Biochemistry 23*, 4624−4630.
49. Tanford, C. (1973) *The Hydrophobic Effect: Formation of Micelles and Biological Membranes*, John Wiley and Sons, New York.
50. Van Lier, J. E., and Smith, L. L. (1970) *J. Org. Chem. 35*, 2627−2632.
51. Nichols, J. W. (1985) *Biochemistry 24*, 6390−6398.
52. Thomas, C. E., and Jackson, R. L. (1991) *J. Pharmacol. Exp. Ther. 256*, 1182−1188.
53. Thomas, J. P., Kalyanaraman, B., and Girotti, A. W. (1994) *Arch. Biochem. Biophys. 315*, 244−254.
54. Steinberg, D., Parthasarathy, S., Carew, T. E., Khoo, J. C., and Witztum, J. L. (1989) *N. Engl. J. Med. 320*, 915−924.
55. Benz, D. J., Mol, M., Ezaki, M., Mori-Ito, N., Zelan, I., Miyanohara, A., Friedman, T., Parthasarathy, S., Steinberg, D., and Witztum, J. L. (1995) *J. Biol. Chem. 270*, 5191−5197.
56. Parthasarathy, S., Santanam, N, Ramachandran, S., and Meilhac, O. (1999) *J. Lipid Res. 40*, 2143−2157.
57. Sattler, W., and Stocker, R. (1993) *Biochem. J. 294*, 771−778.
58. Fluiter, K., Vietsch, H., Biessen, E. A. L., Kostner, G. M., van Berkel, T. J. C., and Sattler, W. (1996) *Biochem. J. 319*, 471−476.
59. Christison, J. K., Rye, K. A., and Stocker, R. (1995) *J. Lipid Res. 36*, 2017−2026.
60. Wirtz, K. W. A. (1991) *Annu. Rev. Biochem. 60*, 73−99.
61. Tyrrell, R. M., and Pidoux, M. (1989) *Photochem. Photobiol. 49*, 407−412.

BI011408R